land

MDPI

Article

Archaeomagnetic Dating of Three Furnaces inside the Middle Age Settlement of San Genesio (San Miniato, Pisa, Italy)

Claudia Principe [1,*], Avto Goguitchaichvili [2,†], Marina Devidze [3], Sonia La Felice [1], Ruben Cejudo [4], Juan Morales [2] and Federico Cantini [5]

[1] Istituto di Geoscienze e Georisorse, Laboratorio di Archeomagnetismo, IGG-CNR, 55049 Viareggio, Italy
[2] Servicio Arqueomagnetico Nacional, Instituto de Geofisica—Campus Morelia, Universidad Nacional Autónoma de México (UNAM), Ciudad Universitaria, 58190 Morelia, Mexico
[3] M. Nodia Institute of Geophysics, Ivane Javakhishvili Tbilisi State University, 0162 Tbilisi, Georgia
[4] Laboratorio Universitario de Geofísica Ambiental, Instituto de Geofísica—Campus Morelia, Universidad Nacional Autónoma de México (UNAM), Ciudad Universitaria, 58190 Morelia, Mexico
[5] Dipartimento di Civiltà e Forme del Sapere, University of Pisa, 56124 Pisa, Italy
* Correspondence: c.principe@igg.cnr.it
† Current address: Geophysics, Department of Physics, University of Alberta, Edmonton, AB T6G 2E1, Canada.

Abstract: Archaeomagnetic dating using full geomagnetic vector was performed on three furnaces cropping out at San Genesio archaeological zone, an ancient settlement located in the Arno River plain, near San Miniato (Pisa). The first evidence of human presence in this area dates back to the period between the VI century BCE and 1248 CE, when the village of San Genesio was destroyed by the inhabitants of the nearby castle of San Miniato. Three burned structures were located at different stratigraphic levels. The SGEN01 represents a kiln to produce pottery. The SGEN02 is probably a furnace for domestic use, while the SGEN03 is interpreted as a metallurgic kiln due to the presence of some hematite fragments possibly coming from Elba Island. Both mean paleodirections and absolute intensity were compared with the global geomagnetic model SCHA.DIF4K (Pavón-Carrasco et al., 2021) for Europe. The obtained age intervals at the 65% probability are 846-911 CE for SGEN01, 696-799 CE for SGEN02, and 623-644 CE for SGEN03. These new absolute dates agree well with their archaeological/stratigraphic position and with the history of the archaeological place.

Keywords: Vicus Wallari; San Genesio; San Miniato; archaeomagnetism; furnaces

Citation: Principe, C.; Goguitchaichvili, A.; Devidze, M.; La Felice, S.; Cejudo, R.; Morales, J.; Cantini, F. Archaeomagnetic Dating of Three Furnaces inside the Middle Age Settlement of San Genesio (San Miniato, Pisa, Italy). *Land* **2022**, *11*, 1936. https://doi.org/10.3390/land11111936

Academic Editors: Paolo Biagi and Elisabetta Starnini

Received: 22 August 2022
Accepted: 19 October 2022
Published: 30 October 2022

1. Introduction and Historical-Archaeological Setting of the San Genesio Area

The San Genesio archaeological site (43°41′30.59″ N, 10°52′58.3″ E) is located in the Arno River alluvial plain (*Basso Valdarno*, which is Italian for Lower Arno Valley, Figure 1), at the foot of San Miniato hills, halfway between the cities of Pisa and Florence. This area was the place of an important settlement during medieval times and has been intensively studied by archaeologists since 2001. The following synthesis of the history of this very important and complex archaeological place is mainly based on the exhaustive work of [1].

The geological framework of the San Genesio area [2] had a strong influence on the positioning and the existence itself of this settlement. San Genesio lies near the confluence of the Elsa River with the Arno River, at the southern margin of the Arno River valley. Its altitude (29 m a.s.l.) still today preserves this area from the flooding of these two important waterways. The San Miniato hills to the south of the village were probably rich in woods, while this portion of the Elsa Valley is characterized by the presence of clayey sediments of the Pleistocene age deposited in an ancient marshy environment. These sediments are often more than 75% clay-rich (units *p* and *p2* in the geological map of Figure 1). As is known, water, wood, and clay are the three elements necessary for the production of ceramics. In addition, the presence of the Arno and Elsa Rivers is a further element that has certainly

favored the passage and the marketing of goods from San Genesio over time, including the products of the furnaces which are the subject of the present work.

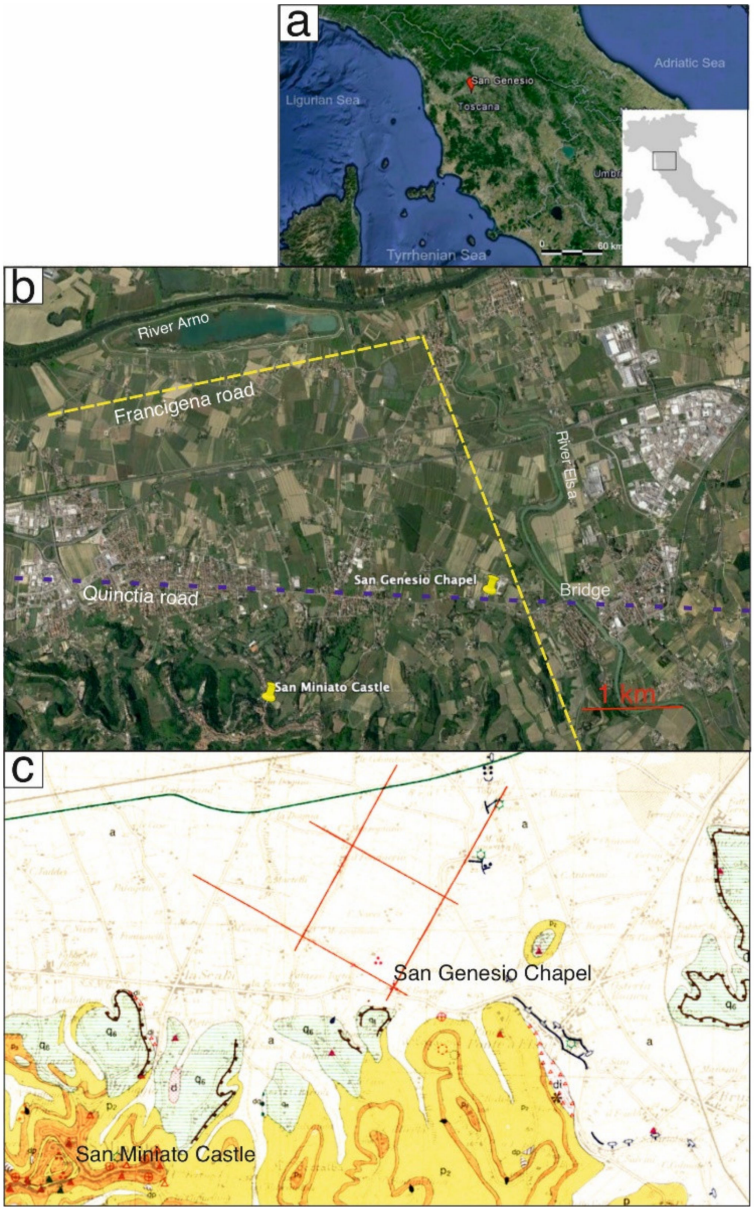

Figure 1. San Genesio location in Tuscany (**a**) and positioning of the archaeological area on Google Maps, at the crossing of the ancient roads *Francigena* and *Quinctia* (**b**) (modified from [3]). The area of San Genesio inside the geological map of [2] (**c**). The red crossed lines in (**c**) correspond to the Roman centuriation traced in 183 BCE [1], of which the archaeological area is located in the southernmost corner.

San Genesio has always had an enviable and strategic position, both militarily and commercially, as it is located (i) more or less at the same distance from the cities of Florence, Lucca, and Pisa; (ii) at the intersection of the Francigena road with the ancient *Quinctia* Roman road, which was built around 123 BCE, perhaps by the consuls *Titus Flaminius* and *Titus Quintus*, to connect the ancient city of Florence (*Florentiae*) with the ancient city of Pisa (*Pisae*) (Figure 1); (iii) not far from the confluence of the rivers Elsa and Arno; and (iv) close to easy crossings of both these waterways, such as the bridge over the Arno whose presence is remembered at least 600 m from today's archaeological site in the 11th century CE (Figure 1). For these reasons, the area in which the San Genesio settlement is located

has always been a peculiar site, rich in resources and more or less always inhabited and exploited from both an agricultural and commercial point of view. It was certainly so (i) in the first Etruscan age, since the middle of the 6th century BCE; (ii) in the Roman period, from the end of the fourth beginning of the 3rd century BCE; and (iii) during the Late Antiquity crisis and the Lombard age, when it was situated at the extreme offshoots of the diocesan territory of Lucca. Throughout the Early and High Middle Ages, San Genesio was one of the most important and well-known parish churches (*Pieve*) of the Lower Arno Valley, which was of great importance in the political strategies of the Lucca episcopate. Later on, the Collegiate Church of San Genesio was visited by the most important personalities of the complex historical period between the eleventh and the thirteenth centuries, which was marked by the growth of the Communes and conflict between the Church and the Empire.

The ancient Roman communication routes, albeit decayed and in large sections compromised, and the wide river valleys guided the penetration of the Germanic populations during the period of the Gothic War, which lasted almost two decades (from 535 to 554 CE) and materialized with the Lombard occupation of this territory following the expedition of Agilulf in central Italy between 593 and 595 CE. This portion of the Arno Valley thus became the border of the Lombard dominion in Tuscany (which is actually the old *Tuscia*, which included more jurisdictions than the present-day Tuscany, especially southward in the current Latium region) and, along this stretch of the river, numerous clashes took place between the Lombards and the Byzantines who lived in the upper portion of the Arno Valley (*Valdarno superiore* and *Mugello* areas). Along this border, a series of military villages ("*vici militares*") were born, the memory of which is still present today in the toponymy of clearly Lombard origin of some places. From the Lombard domination also derives the belonging for a long time of this portion of Lower Arno Valley to the diocese of Lucca, as Lucca was the capital of Lombard Tuscany. The area of interest experienced a period of total or partial abandonment between the 5th and the early 6th century CE, when only the presence of Roman–Byzantine populations is testified and the area was mainly used as a cemetery [4]. Then, the area of interest was repopulated under the Lombard rule at the end of the 6th century CE. This territory was controlled by a Lombard character named Wallar, perhaps an official of the Lucca court, from whose name also comes the ancient toponym of this settlement "*Vicus Wallari*".

During the first half of the 7th century CE, the site of San Genesio seems to have been the subject of another, at least partial, abandonment. However, the first written evidence of the existence of a church and a village of some importance in this place dates back to 714 CE, from which the site will henceforth take the name of San Genesio, which is still preserved today: "*Sancti Ginesii, in vico qui dicitur Walari*" (San Genesio in the village that people name Wallari) [5]. This first church, datable at least to the end of the 7th century CE, was later (presumably during the mid-8th century CE) replaced by a new three-nave structure that was found during archaeological excavations under the remains of a later and more complex ecclesiastical building, datable to the first half of the 11th century.

Until the middle of the eighth century CE, the parish church of San Genesio remained directly under the bishopric of Lucca. Starting from the 770s–780s of the 8th century CE, following the conquest of these territories by the Franks, the bishop introduced concessions in "benefit" to private individuals in some way related to him. Even the parish church of San Genesio with the territory controlled by it suffered this fate. In fact, even the name of San Genesio appears in the "*Breve de Feora*" (dated between 890 and 900 CE), which lists these benefits. In the 10th century CE, the parish church of San Genesio, around which a small urban agglomeration was born at the beginning of this century, is counted among the main "*ecclesiae baptismales*" of that part of the diocese of Lucca which was located south of the Arno River.

In the 10th century CE, the castle of San Miniato, located on top of the hill overlooking San Genesio, grew in importance. The castle of San Miniato became the permanent residence of a vicar of the German emperor, and, on several occasions, the emperors (e.g., Henry III) stopped in San Miniato on their way to Rome. San Miniato thus became a direct

dependence of the empire, and, as testified by written sources, at least from the first half of the 11th century, the inhabitants of San Genesio and the whole territory belonging to its parish paid taxes to the owners of the San Miniato castle, even when the parish remained under the control of the bishop of Lucca.

The transformation of the church of San Genesio into a larger and more complex building with a crypt and frescoes dates back to the same period, i.e., the first half of the 11th century. At the same time, the Lucca curia promoted the creation of a rectory with a rectangular cloister next to the new church, thus transforming the original parish church into a monastic complex ("Collegiata") around which the medieval village developed. These expansion works prelude to a long period of domination of San Genesio, both on the religious structures of San Miniato and on just under 40 chapels and rectories distributed in this area. This period of splendor lasted until the end of the 12th century, as sanctioned by a privileged act of Pope Celestino III dated 24 April 1194. During the various political vicissitudes that followed one another in this period, on the one hand, the importance of San Miniato as a center of imperial power grew, on the other hand, all the important meetings between the various protagonists of medieval life, including popes and emperors, took place in San Genesio for its strategic position at the crossroads of the most important communication routes. Towards the end of the twelfth century, hatred between San Genesio and San Miniato was born and fueled, due to the political conflicts between the Papacy and the Empire and between the various Tuscan Communes that side with one or the other. The decline of San Genesio began in conjunction with the events that led to the signing of the Guelph League between the Tuscan Communes against the Emperor in 1197. However, it was Emperor Frederick II who marked the fate of San Genesio, first transforming the castle of San Miniato into one of the key strongholds of the defensive system of Florence and then establishing, with an act issued in 1216, the submission of San Genesio to San Miniato. Although in 1240 San Miniato lost the dominion of San Genesio and the favor of the emperor, in 1248, the inhabitants of San Miniato razed San Genesio to the ground. From that moment, the dominion of Lucca over this part of the lower Arno Valley ended. The ancient village of San Genesio was never rebuilt, and only the written memory remains of the past splendor, while the memory of this place fades. At the time of the systematic archaeological excavation, the San Genesio area was occupied only by crops and a small chapel built in the nineteenth century.

Three furnaces were excavated during the archaeological surveys. They are positioned at different geometric and stratigraphic levels within the excavated area and were ascribed to different types of use. From top to bottom, the SGEN01 furnace, positioned inside the stratigraphic unit US-29172, was labeled as activity structure n. 102, and interpreted as a ceramic kiln. The SGEN02 furnace, situated in the stratigraphic unit US-37129, was called activity structure n. 399, while the SGEN03 furnace (US-38119; activity structure n. 662) was interpreted as a metallurgic structure due to the presence of some hematite fragments, possibly coming from Elba Island, inside it. The aim of the present work was to position these three structures within the local chronostratigraphy summarized above. This aim was achieved through the archaeomagnetic analysis method and was made possible by the recent and impressive improvement of the reference paleomagnetic curves for the medieval period [6–9].

2. Archaeomagnetic Sampling

Oriented hand samples (Figure 2) were obtained using the Modified *Thellier* Sampling Technique already described in [10]. The main modification to the classical Thellier's method [11] consists in a preliminary surrounding of the samples with plastered bandages. This technique allows one to collect a greater quantity of materials with a low risk of movement of fine particles. For example, the blocks of baked clays sampled during this work have an average dimension of 8 cm × 8 cm × 4 cm. Then a plaster cap with a perfectly horizontal plane was superposed on the sample using a precision level (Figure 2). A total of 47 (Tables 1–3) independently oriented samples were collected (16 from SGEN01, 16 from

SGEN02, and 15 from SGEN03), using both a magnetic compass and a sun compass, and marked with reference directions on the large (6–8 cm in diameter) plaster caps.

Figure 2. Sampled structures. (**a**–**c**): The plane of ca. 80 × 30 cm of SGEN01 ceramic furnace. (**d**,**e**): Sampling the plane (ca. 70 × 50 cm) of the SGEN02 furnace, probably a domestic structure. (**f**): Building a perfectly horizontal plane for the accurate orientation with a solar compass on top of the plane (ca. 30 × 25 cm) of the SGEN03 metallurgic furnace.

Table 1. Sampling and Directional data: Analytical results SGEN01.

Subset	**Sample**	**Dec (°)**	**Inc (°)**	**VRM %**	**Dec (°)**	**Inc (°)**
01	04	5.2	65.0	9.5	7.8	65.3
01	05	9.4	62.8	5.3	12.0	62.9
01	07	11.6	64.1	8.7	9.3	64.3
01	08	6.4	65.3	7.3		
01	09	9.4	66.3	8.3	8.9	66.6
01	10	15.4	65.7	10.1	8.7	66.1
01	11	11.8	66.6	7.9	12.3	66.8
01	12	8.9	69.0	7.7	12.4	69.2
01	13	17.0	66.4	7.8	14.0	67.6
01	14	15.4	67.6	7.6	12.6	68.1
01	15	18.4	67.2	4.7	19.8	67.8
01	16	18.4	67.0	4.1	20.3	66.7

Mean directions

Subset	Lat. (°N)	Long. (°E)	n/N	Dec (°)	Inc (°)	k	α^{95}	VRM %
SGEN01	**43.69**	**10.88**	**12/16**	**11.9**	**66.4**	**107**	**1.2**	**7**

Table 2. Sampling and Directional data: Analytical results SGEN02.

Subset	Sample	Dec (°)	Inc (°)	VRM %	Dec (°)	Inc (°)
02	01	−0.9	67.6	14.0		
02	02	0.0	66.6	5.7		
02	03	14.4	66.3	4.9	15.0	66.8
02	04	−7.2	68.1	6.2		
02	05	0.9	72.0	9.5		
02	06	4.9	65.5	8.0		
02	07	0.1	68.4	7.9		
02	08	3.2	68.4	7.3		
02	09	−2.4	71.8	15.3		
02	11	−0.9	68.0	8.6		
02	12	1.9	64.9	6.4	0.4	63.7
02	13	5.3	63.5	12.7		
02	14	0.6	65.4	5.1		
02	15	−4.2	68.8	13.3		

Mean directions

Subset	Lat. (°N)	Long. (°E)	n/N	Dec (°)	Inc (°)	k	α^{95}	VRM %
SGEN02	**43.69**	**10.88**	**14/16**	**1.2**	**67.5**	**639**	**1.5**	**8.9**

Table 3. Sampling and Directional data: Analytical results SGEN03.

Subset	Sample	Dec (°)	Inc (°)	VRM %	Dec (°)	Inc (°)
03	01	−7.7	63.6	2.9	−8.6	63.2
03	02	1.8	64.6	2.8	−1.5	64.7
03	04	−0.1	66.2	2.9	−1.1	67.3
03	05	−3.3	65.0	2.9	−4.0	65.3
03	06	3.1	64.6	2.9	1.1	65.7
03	09	−6.5	64.3	2.3	−8.2	63.1
03	10	1.5	62.1	4.0	−2.5	62.9
03	11	−1.8	63.6	2.6	−3.5	62.8
03	12	−4.5	63.2	2.6	−4.5	63.2
03	13	−1.0	63.6	3.1	−1.4	63.8
03	14	−4.5	64.9	3.9	−4.4	64.9
03	4BIS	−1.5	65.2	2.9	−3.5	64.6
03	7BIS	−12.6	64.3	5.9	−6.9	63.6

Mean directions

Subset	Lat. (°N)	Long. (°E)	n/N	Dec (°)	Inc (°)	k	α^{95}	VRM %
SGEN03	**43.69**	**10.88**	**13/15**	**−3.5**	**64.3**	**2090**	**0.8**	**3.2**

3. Laboratory Proceedings

Directional measurements (Tables 1–3) were performed on all 47 sampled clay fragments by means of the large cell induction magnetometer of the Saint Maur des Fossés Laboratory (Institute de Physique du Globe de Paris) in Paris [12]. Perfect plaster cubes (12 cm × 12 cm × 12 cm) were introduced into the magnetometer while the pre-analytical database was prepared in the Archaeomagnetic Laboratory of IGG-CNR at Villa Borbone, Viareggio (Italy). The archaeointensity measurements and magnetic mineralogy experiments were carried out at the facilities of the Servicio Arqueomagnetico Nacional of UNAM in Morelia (Mexico).

4. Directional Analyses

A preliminary viscous remanent magnetization cleaning was performed [13]. The procedure consists of storing the samples for about 20 days in a free magnetic shield before magnetic measurements. After that, the same procedure was repeated after reversing the samples by 180°. In this way, the index of the acquired viscous remnant magnetization

(VRM) could be estimated and subtracted to the full TRM (thermoremanence magnetization) vector. In the case of the San Genesio analyses, the VRM index resulted in quite high mean values of 7.4% (SGEN01), 8.9% (SGEN02), and 3.2% (SGEN03). Samples yielding a magnetic viscosity index >15%, as defined by the VRM/TRM ratio, were rejected from further procedures.

In order to retrieve the primary characteristic of the remanent magnetization, samples were demagnetized by employing alternating fields (AF), up to a maximum AF peak of 40 mT. The remanent magnetizations were measured after each demagnetization step (Figures 3 and 4). Representative demagnetization diagrams for SGEN01-14 and SGEN03-04 samples are reported in Figure 3. Samples from the SGEN02 structure are characterized by a relatively weak remanent magnetization. For this reason, the AF demagnetization procedure was fully applied only to the sample SGEN02-12, which shows a linear demagnetization segment (Figure 4b).

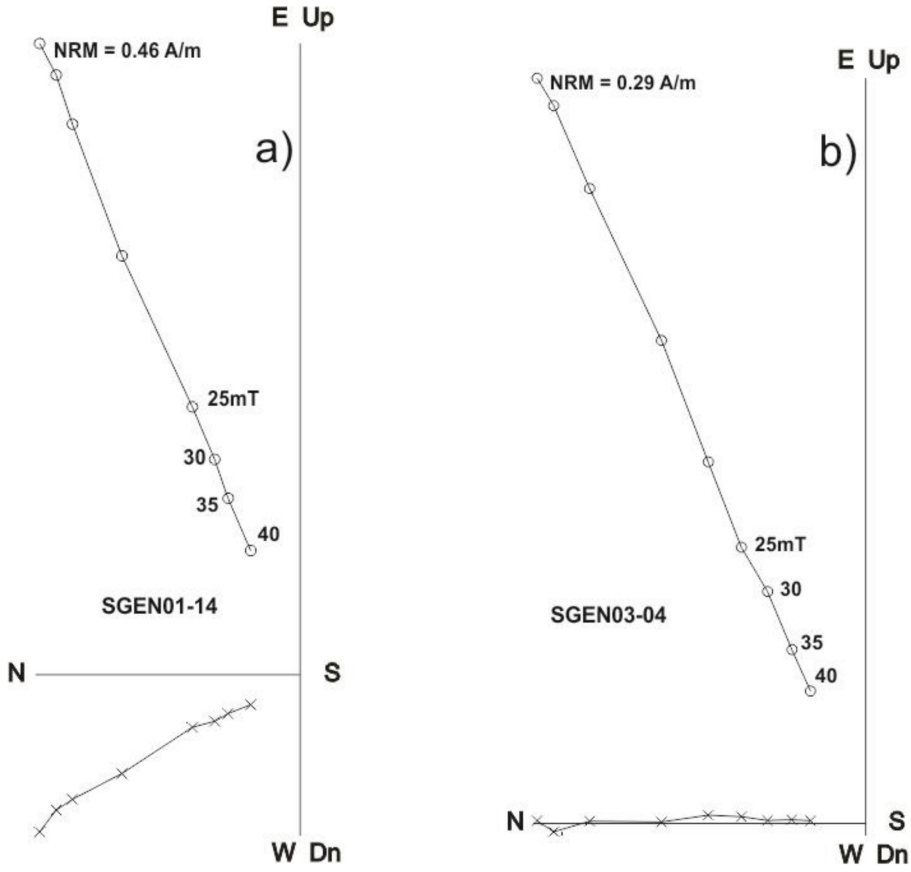

Figure 3. AF demagnetization curves for selected samples. See text for the explanations.

The demagnetization trends of most samples from the SGEN01 site show a lowering of the declination values with increasing demagnetization peaks (Figure 4a). This fact implies that few samples had to be discarded, as they moved outside the McFadden confidence circle [14]. This behavior can be interpreted as due to either unstable magnetic mineralogy or to a displacement of the kiln during past times. As anticipated, the baked clays from the plain of the SGEN02 furnace show a very low magnetization. This fact is particularly evident in the samples characterized by the presence of less-colored clay, as, for instance, samples SGEN02-1,9,10,15,16 (Figure 2). In these samples, the lack of red color for a portion of the sampled clays probably correspond to a lower heating degree and, consequently, the absence or deficiency of iron oxidation, which is the process responsible for the red color. In the majority of the samples from the SGEN03 furnace, an unstable secondary component between NRM and 5–10 mT is quite evident, while the characteristic remanent

magnetization (CHRM) was successfully isolated from 10 mT upward, where a linear segment trending toward the origin of the orthogonal projection was defined (Figure 3).

As a general statement, a reliable archaeomagnetic age depends on two main factors. They are (i) good statistics, resulting in low values of the α_{95} parameter (the semi-angle of confidence of the conic surface that collects all the directional measurements) and high values of the k-precision parameter [15] and (ii) the use of a valid reference curve (PSVC) or a portion of it [6–9,16,17]. The accurate sampling methodology and the high number of independent, big-size, solar-oriented samples (N = 15–16) resulted in good analytical statistics for the San Genesio furnaces, with α_{95}/k values of 1.23/1077 (SGEN01), 1.48/639 (SGEN02), and 0.85/2090 (SGEN03) (Tables 1–3). The relatively low α_{95} value of the SGEN02 furnace is particularly valuable when considering the low magnetization of the baked clays of this structure.

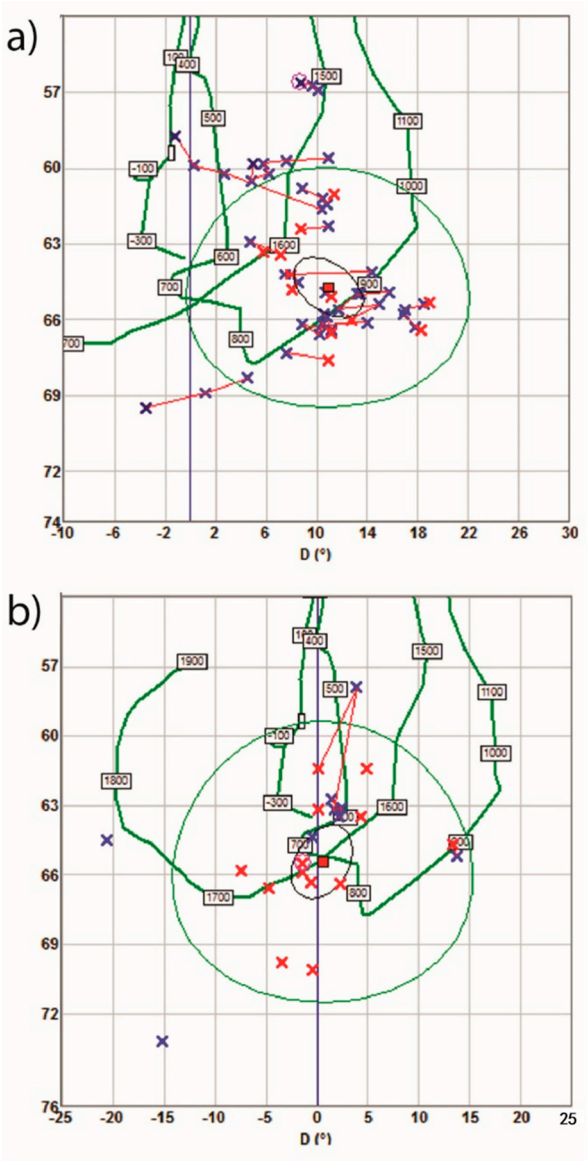

Figure 4. *Cont.*

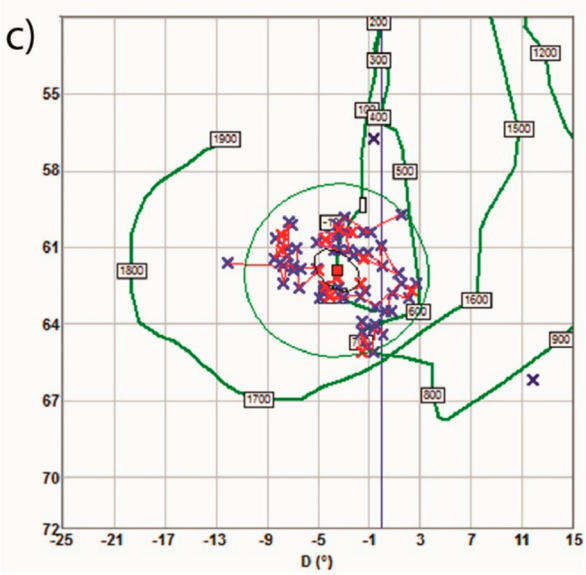

Figure 4. Graphic outputs of the Saint Maur des Fossés large cell inductometer for (**a**) SGEN01; (**b**) SGEN-02; (**c**) SGEN03. The AF demagnetization patterns of each specimen are shown. The green [14] circles of confidence are also shown. Degrees of inclination of the TRM vector are reported on the vertical axis. Declination degrees are on the horizontal axis. The geomagnetic secular variation curve reported, for graphical preliminary age indication, is that of [18].

5. Archaeointensity Determinations

Three virgin fragments of the sampled clays have been used for intensity measurements. They are one fragment of the SGEN01 (13 samples) and two fragments of the SGEN03 (14 samples).

Samples were prepared in three different ways, according to the process to be applied. A small specimen (~1 cm × 1 cm) from each studied fragment was cut, placed, and fixed inside a 1″ plastic cubic sample holder to facilitate its alternating field demagnetization treatment. Chips from each of the available fragments were crushed and pulverized with an agate mortar and pestle to obtain approximately 250 mg for use with the advanced variable field translation balance (AVFTB). For the archaeointensity measurements, fragments were broken into at least 6 specimens and pressed into salt pellets to facilitate their treatment as standard paleomagnetic cores. Specimens (belonging to the same fragment) were positioned into the pellets in six different directions (+X, −X, +Y, −Y, +Z, −Z), relative to the a priori chosen direction of the shard to minimize or mitigate the thermoremanent magnetization anisotropy effects. All remanences were measured with a JR6a spinner magnetometer, while isothermal remanent magnetization (IRM), hysteresis loops, backfield, and high-temperature thermomagnetic curves were obtained using an advanced variable field translation balance (also known as the Curie Balance). In some cases, susceptibility vs. temperature continuous curves were recorded using an AGICO Kappa-bridge magnetic susceptibility meter equipped with a furnace.

The Thellier–Coe method [13,19,20] was used for the ancient field determinations procedure. This is a very standardized procedure but is reported here below for completeness. Samples were heated and cooled in air using an ASC Scientific TD48-SC furnace. Fifteen temperature steps were distributed from room temperature to 585 °C. During the in-field steps of the protocol, a laboratory DC magnetic field of (50.0 ± 0.05) μT was applied during heating and cooling along the *z*-axis of the cylindrical samples. Every third temperature step, a pTRM check (control heating) was performed to detect possible changes in the pTRM's acquisition capacity. The cooling rate dependence of TRM was investigated following a modified procedure to that described by [21]. At the end of the AI experiments, all specimens were heated two more times at 560 °C under the same laboratory field. The

last measurement (in-field step) of the AI experiment was designated as TRM1. Then, a second TRM (TRM2) was given to all the samples but this time using a longer cooling time (~6 to 7 h). Finally, a third TRM (TRM3) was created using the same cooling time as that used during the TRM1 creation (~40 to 45 min). The cooling rate factor f_{CR} was calculated as the ratio between the intensity acquired during a long and a short cooling time: f_{CR} = TRM2/TRM1. Changes in TRM acquisition capacity were estimated through the percentage variation between the intensity acquired during the same cooling time (f_{AC} = TRM3/TRM1). The cooling rate correction was only applied when the corresponding change in TRM acquisition capacity was close to 1 and $f_{CR} > 1$ [22].

In total, 19 samples (Table 4) yielded technically acceptable paleointensity determinations. For these samples, the NRM fraction *f* ranges between 0.86 and 0.61, while the quality factor *q* varies from 6.8 to 14.4. The individual archaeointensity values obtained in this study range from 35.7 to 71.2 μT, with medium values of 38.7 μT for SGEN01/13 and 66.1 μT and 67.8 μT for the two fragments of SGEN03/14.

Table 4. Summary of archaeointensity determination with Coe et al., 1978, including quality parameters together with interval of temperatures involved.

SAMPLE	LAB REF	N	T1-T2	f	g	q	H(anc)	σH
SGEN01/13	51	12	200-585	0.62	0.82	9.6	37.6	1.2
	52	13	150-585	0.61	0.83	9.2	40.7	2.1
	53	13	150-585	0.56	0.86	7.6	43.6	2.2
	54	13	150-585	0.72	0.84	10.3	38.6	2.5
	55	12	200-585	0.73	0.81	11.2	38.4	2.2
	56	12	200-585	0.69	0.82	8.3	36.5	2.1
	57	13	150-585	0.74	0.84	12.6	35.7	1.9
							38.7	**2.7**
SGEN03/14A	60	13	150-585	0.81	0.87	14.4	63.1	3.1
	61	11	250-585	0.80	0.85	9.3	64.4	3.2
	62	11	250-585	0.74	0.81	6.8	66.1	3.4
	63	12	200-585	0.82	0.83	14.1	67.2	3.9
	64	11	250-585	0.79	0.82	11.2	69.6	4.1
	65	12	200-585	0.86	0.86	14.8	68.1	4.2
							66.1	**2.9**
SGEN03/14B	66	11	250-585	0.83	0.88	14.3	71.2	4.3
	67	11	200-575	0.79	0.83	11.1	68.2	4.2
	68	11	250-585	0.85	0.84	15.8	67.4	4.3
	69	11	250-585	0.82	0.84	12.6	68.8	4.1
	70	11	250-585	0.78	0.80	8.9	66.7	3.9
	71	12	150-575	0.79	0.52	8.2	65.6	4.5
							67.8	**1.9**

The main concern during any absolute-intensity study is related to the uncertainty of whether the technically determined values have geomagnetic significance and thus confirm the primary thermoremanent origin of the magnetization created in these samples during the cooling from high temperatures. Most representative Arai–Nagata plots are presented in Figures 5 and 6. In both cases, the determinations seem to be of high technical quality. Associated saturation magnetization vs. temperature curves yielded reasonably reversible heating and cooling segments pointing to Ti-poor titanomagnetite (almost pure magnetite) as the principal magnetic carrier. The continuous susceptibility plot, however, shows marked irreversibility for sample SGEN01 (Figure 7) with evidence for two ferromagnetic phases during the heating, while the cooling curve only indicates the presence of magnetite. This behavior may be due to the inversion of unstable titanomaghemites into magnetite, and, thus, the remanent magnetization may be suspected to have chemical or thermochemical remanent magnetization [23]. Due to this fact, the intensity value of sample SGEN01 was not used for the archaeomagnetic-dating exercise, and probable age intervals were estimated based only on magnetic inclination and declination. The susceptibility

vs. temperature curve for sample SGEN03 shows reversible behavior during the heating–cooling cycle and indicates evidence of a single ferromagnetic phase (magnetite) on both segments. In this case, the archaeomagnetic dating was achieved using the full geomagnetic vector (direction and intensity). As already proved by [24], continuous susceptibility curves appear more sensitive to magnetic mineralogy than directional ones, which agrees with theoretical considerations. Magnetic susceptibility thermal variation combines the thermal variation of the two magnetic parameters (spontaneous magnetization, Ms, and coercive force, Hc) when induced magnetization (i.e., when saturation is reached) describes the thermal evolution of spontaneous magnetization only.

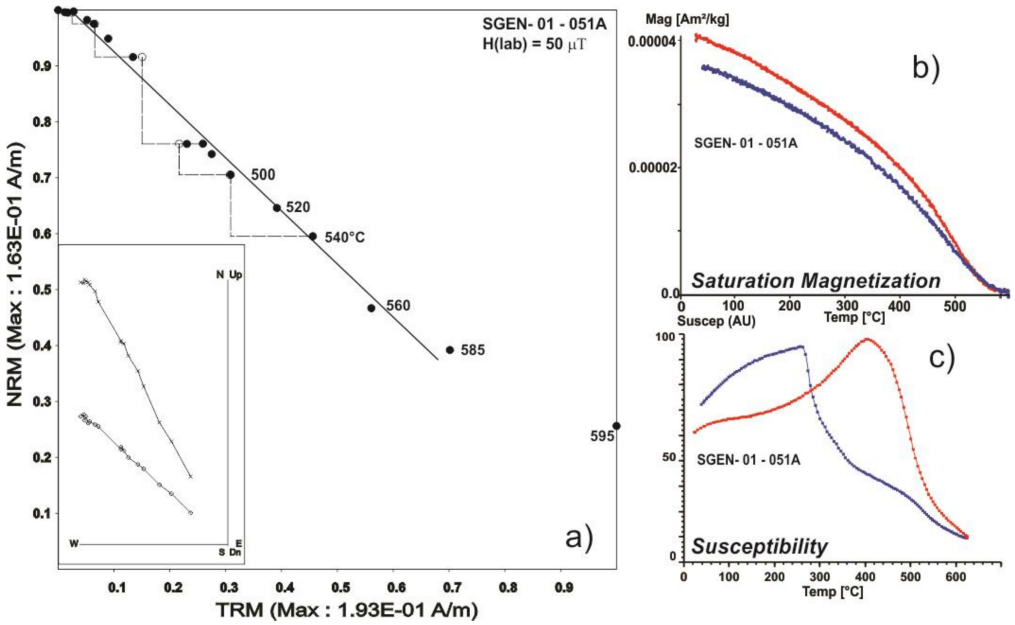

Figure 5. Thellier–Coe paleointensity determination for sample SGEN01 together with associated NRM endpoint (**a**) orthogonal vector plot. Also shown are saturate magnetization (**b**) and susceptibility (**c**) vs. temperature continuous thermomagnetic curves.

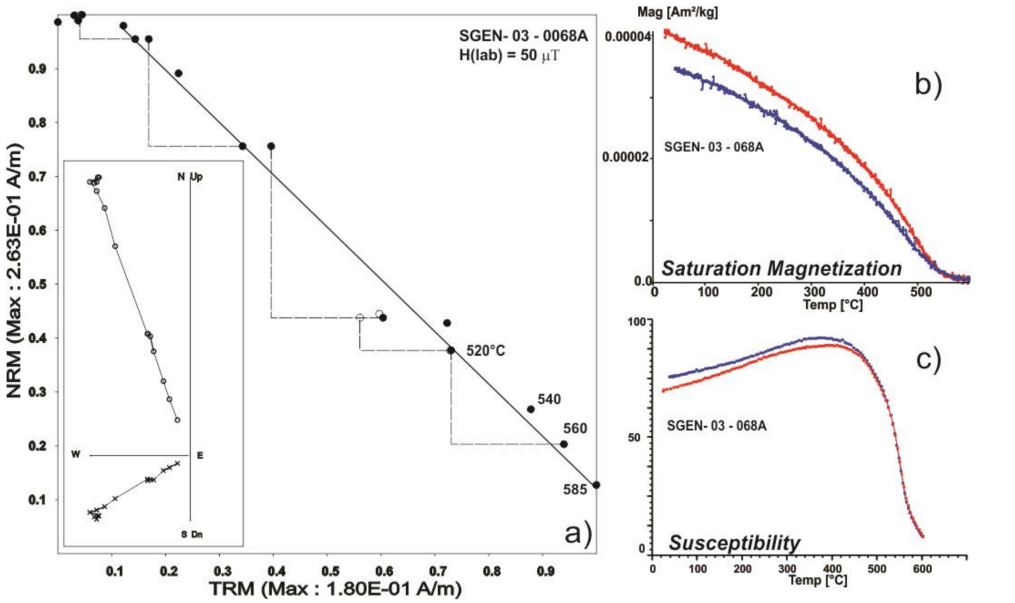

Figure 6. Thellier–Coe paleointensity determination for sample SGEN03 together with associated NRM endpoint (**a**) orthogonal vector plot. Also shown are saturate magnetization (**b**) and susceptibility (**c**) vs. temperature continuous thermomagnetic curves.

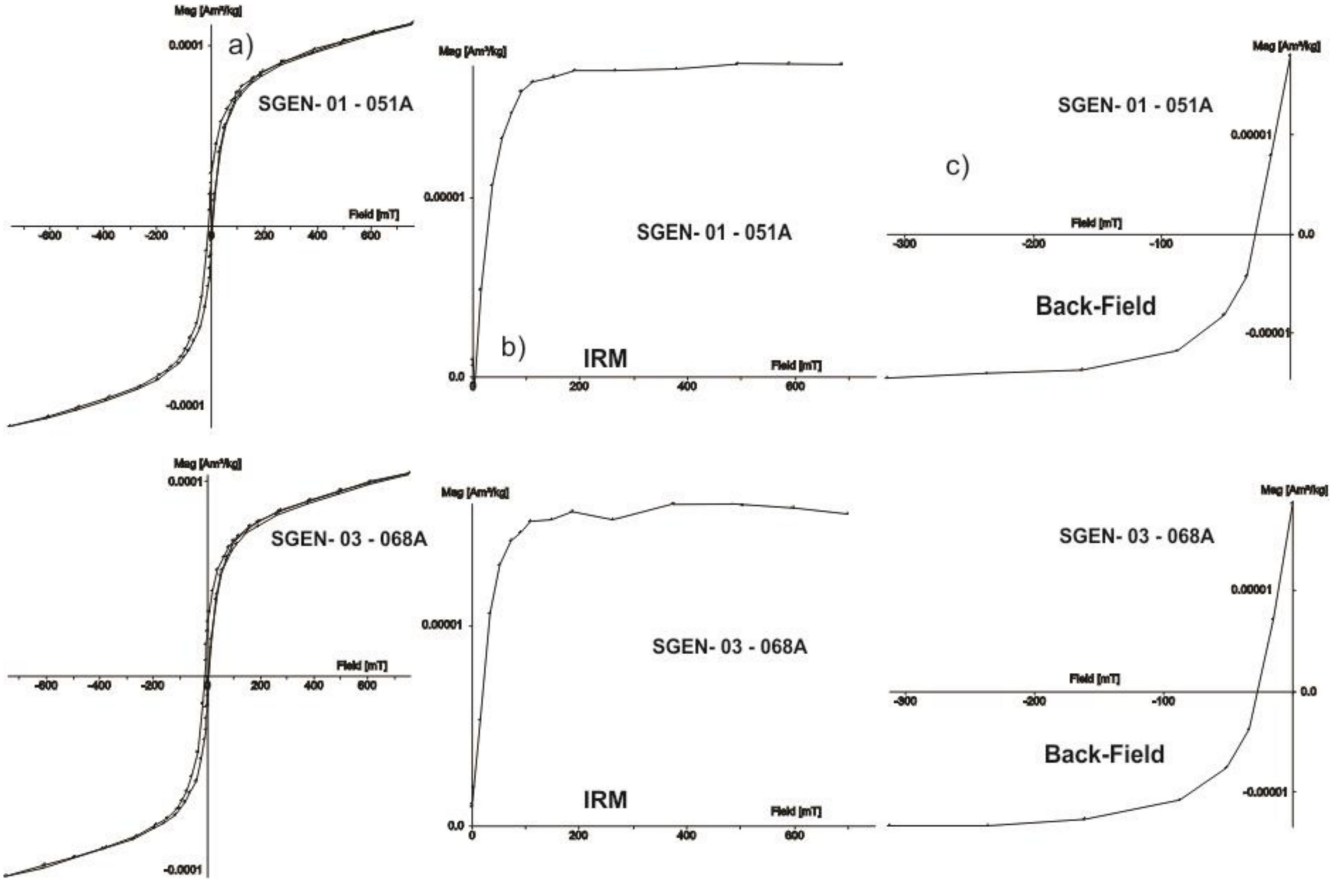

Figure 7. A summary of rock-magnetic experiments carried out on San Genesio samples: (**a**) hysteresis plot obtained with variable field translation balance, (**b**) associated isothermal-remanent acquisition curve, and (**c**) back-field experiments to retrieve the coactivity of remanence.

6. Archaeomagnetic Ages

The directional and intensity measurements on the three San Genesio furnaces were processed using the SCHA.DIF.4k model proposed by [6], which is the most complete PSVC currently available for Europe. The resulting ages for the analyzed structure are SGEN01: 855–987 CE at the 95% probability level and **846–911 CE** at the 65% probability level; SGEN02: 651–848 (95%), **696–799 CE** (65%). The SGEN01 ceramic furnace results indicate a younger and larger age interval compared to the one obtained by the 6.0 version of the PSVC curve [8] (Table 5). This fact is due to the flat top (Figure 8) of the updated reference geomagnetic curve SCHA.DIF.4k, which is used in the 8.0 version of the MATLAB tool for archaeomagnetic dating produced by [7]. The same effect (Table 5 and Figure 9) takes place for the age range of SGEN02, which is widened compared to the age previously obtained with the second version of the curve [9].

Table 5. Directional ages calculated from different versions of the PSVC. (1) SHA.DIF.14k model [7]. (2) SCHA.DIF.4k model [9].

	(1)	(2)
SGEN01	759–849 CE	**846–911 CE**
SGEN02	680–721 CE	**696–799 CE**
SGEN03	624–631 CE	**623–644 CE**

The obtained directional age for the SGEN03 furnace is 611–676 CE (at the 95% probability level) and **623–644 CE** at the 65% probability level (Table 5). By adding the mean of intensity data obtained from the analysis of two fragments of the same furnace, a value of

621–650 CE is obtained with a 95% probability level using both directional and intensity curves of [7,8], and a value of 624–631 results at the 65% probability level (Table 5 and Figure 10a). We processed SGEN03 data also with the reference curve of [9], but the still imprecise intensity curve available for this time interval [8] in the version 8.0 of the dating tool resulted in a loss of precision of this datum. For this reason, we accept here the only directional and slightly less precise age obtained by the 8.0 version of the dating tool (Figure 10b). This choice is reasonable also considering that the high precision of the data obtained for this furnace (α_{95} 0.8) requires an equally precise reference curve to obtain a reliable age.

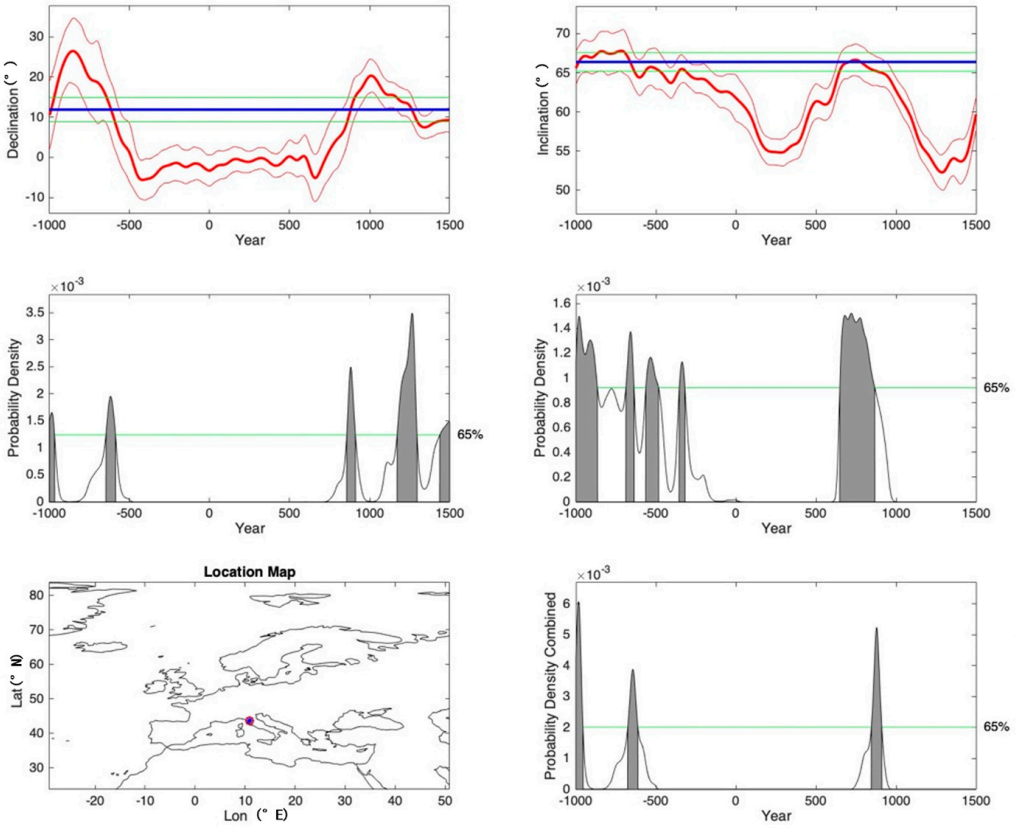

Figure 8. Archaeomagnetic dating of the SGEN01 furnace. Inclination and declination curves are shown with their probability density. The SCHA.DIF.4k model proposed by [9] has been used. Calibrated date intervals are given at a 65% level.

As we have seen (Table 5), the obtained ages based on the new version of the dating tool [9] differ slightly from the directional ages previously obtained by the use of older, less complete reference curves [7]. In fact, absolute ages depend on the adopted reference curve, and these two pieces of information should always be considered together. Furthermore, the perfect curve for describing changes in directional and intensity geomagnetic values can only be drawn for the period after 1640, when direct measurements of the earth's magnetic field began [25]. Of course, also for this curve, the uncertainties decrease with the increase in the number and precision of the measurements made over time by scholars of magnetism. For the previous periods, it is necessary to rely totally on reference curves built on data obtained from measurements made on objects of known age, obtained in another way. For this reason, the geomagnetic reference curves have varied a lot over time and, consequently, also the age determinations that were based on these varying reference curves.

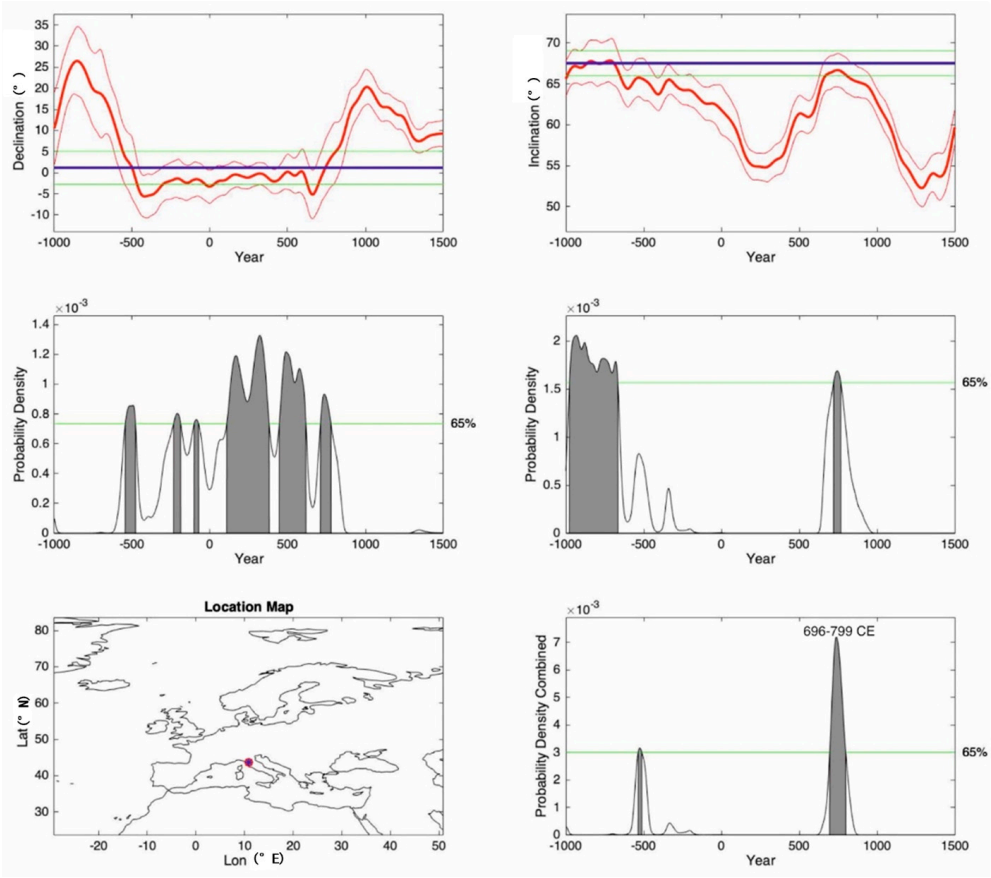

Figure 9. Archaeomagnetic dating of the SGEN02 furnace. Inclination and Declination curves are shown with their probability density. The SCHA.DIF.4k model proposed by [9] has been used. Calibrated date intervals are given at a 65% level.

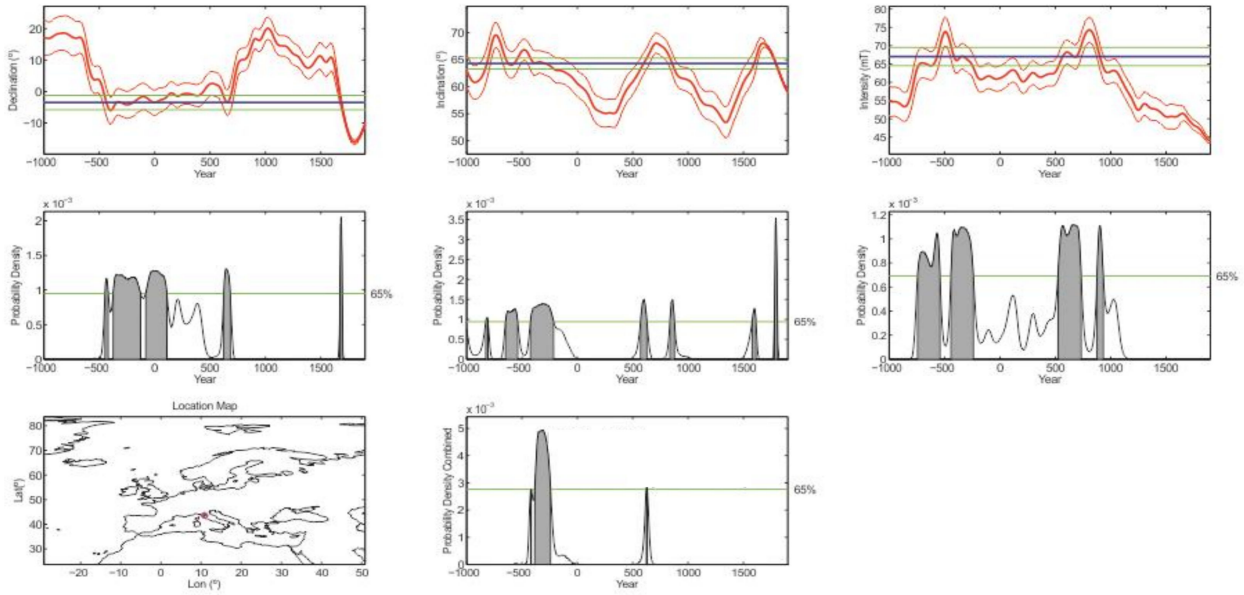

(**a**)

Figure 10. *Cont.*

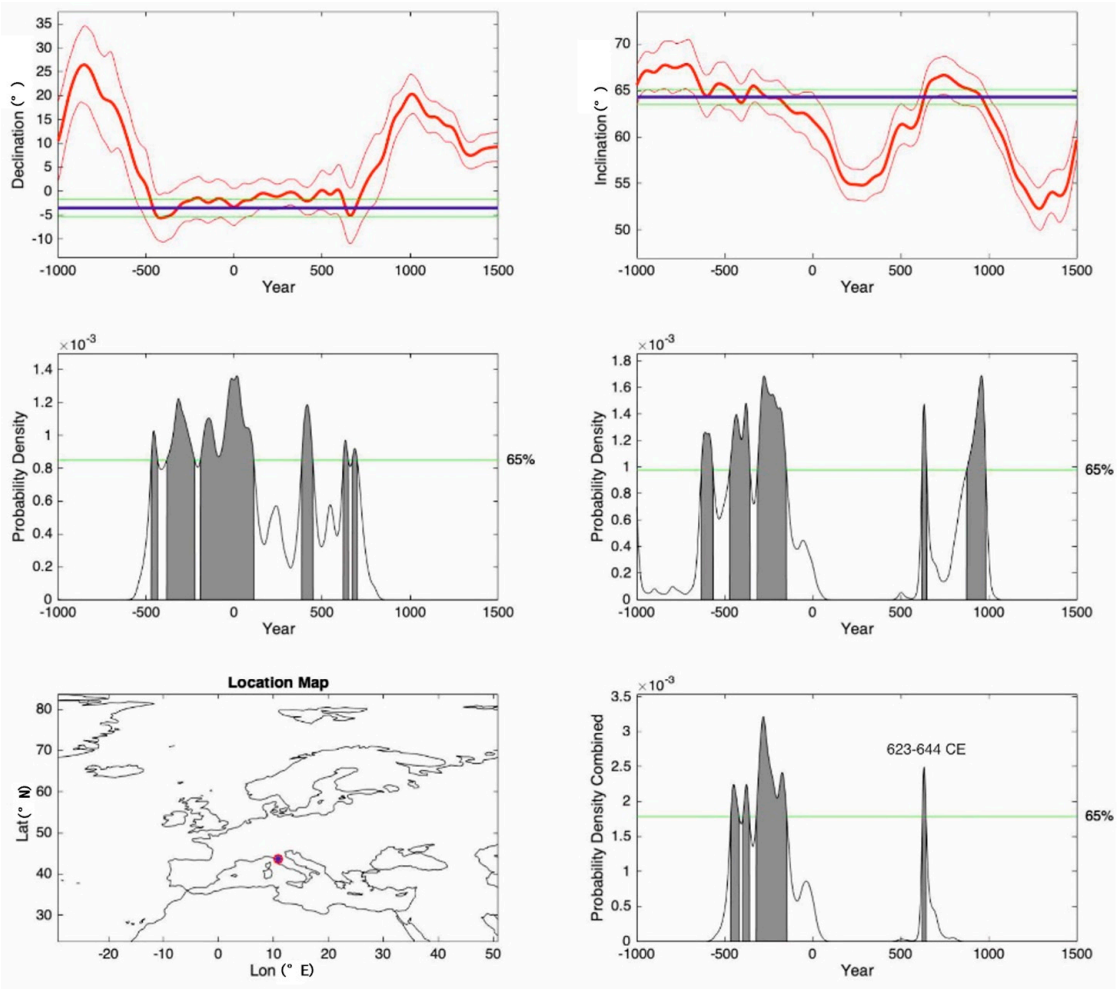

Figure 10. (**a**)—Archaeomagnetic dating of the SGEN03 furnace. Full vector curves are shown with their probability density. SHA.DIF.14k model proposed by [7] has been used. Calibrated date intervals are given at a 65% level. (**b**)—Archaeomagnetic dating of the SGEN03 furnace. Inclination and declination curves are shown with their probability density. The SCHA.DIF.4k model proposed by [9] has been used. Calibrated date intervals are given at a 65% level.

7. Data Discussion and Conclusions

At the transition between the 9th and 10th centuries CE, the settlement built around the San Genesio parish church was a place of passage and rest for numerous travelers due to its location at the intersection between the Via *Francigena* and the *Quintia* [1]. Thus, the presence of a ceramic kiln used for the production of pottery is expected in this time period, consistent with the age interval of furnace SGEN01, from 846 to 911 CE with a probability of 65%. The SGEN02 furnace shows the largest age interval, from 696 to 799 CE with a probability of 65%, among the three analyzed structures. This result could be due to the higher analytical uncertainty, with α_{95} of 1.5, compared to the other two furnaces SGEN01 and SGEN03, with α_{95} of 1.2 and 0.8, respectively. In turn, these higher analytical uncertainties can be related to the feeble magnetization of the clay used for building this furnace, as suggested by the obtained results and the partial lack of red color. The 8th century CE corresponds to the more probable period for the first reconstruction and enlargement of the parish church of San Genesio (which will be cited from this moment on as "ecclesia Sancti Genesii" in the latin written sources) when perhaps it was decided to promote it as a baptismal church ("*ecclesiae baptismales*"), a title that was found in documents starting from 763 [1]. It is very probable that this period also corresponds to a growth of the inhabited area and consequently of service structures, such as shared domestic ovens, as the structure of SGEN02 could be tentatively interpreted.

In the San Genesio area, four major funerary phases have been recognized [26,27]. The first one (Late Antique) has been dated to the 6th century CE and is the oldest cemetery phase recorded at this site. The second one (Early Medieval I) dates to the 7th–9th century CE, while the third phase (Early Medieval II) dates to the 10th century CE [4]. The fourth and last phase (Late Medieval) spans from the 11th to the 13th centuries. In this framework, the SGEN03 furnace is of interest for the presence of graves curved inside the furnace itself (Figure 2). The archaeomagnetic directional age estimated for the SGEN03 structure (from 623 to 644 CE with a probability of 65%) is the most precise of the obtained ages in the studied area. The obtained age range for this furnace positions this structure before the presence of the first ecclesiastical structure at San Genesio (the second half of the 7th century AD) and at the beginning of the second of the known funerary phases. Furthermore, the age and the metallurgic use of this furnace are consistent with the archaeological investigation that has attested the presence of craft activities during this period [1,4].

In conclusion, this archaeomagnetic study allowed us to give an age to three furnaces belonging to three distinct phases of frequentation and use of the site of San Genesio, which agreed with their stratigraphic order and the very complex overlap of structures and memories that characterized this important archaeological place during times.

Author Contributions: Conceptualization, C.P. and F.C.; methodology, A.G., R.C., J.M.; software, A.G.; formal analysis, C.P., A.G., M.D., S.L.F., R.C., J.M.; investigation, C.P., F.C.; resources, A.G.; data curation, C.P., A.G., M.D., S.L.F., R.C., J.M.; writing—original draft preparation, C.P., A.G., M.D., S.L.F., R.C., J.M.; writing—review and editing, C.P., A.G., M.D., S.L.F., R.C., J.M., F.C.; All authors have read and agreed to the published version of the manuscript.

Funding: This research received no external funding. AG acknowledges the financial support given by UNAM-DGAPA during the sabbatical stay.

Data Availability Statement: All data produced for this work are reported inside this paper.

Acknowledgments: The authors wish to thank Maxime Le Goff of the IPGP Saint Maur des Fossés Laboratory for the assistance during the lab analyses in Paris, and Tsegaye Abebe Adhana for the help in sample handling before the analyses. J.F. Pavón-Carrasco and two anonymous reviewers are acknowledged for their valuable help in improving the manuscript.

Conflicts of Interest: The authors declare no conflict of interest.

References

1. Cantini, F.; Salvestrini, F. *Vico Wallari—San Genesio, Ricerca e Indagini Archeologiche su una Comunità del Medio Valdarno Inferiore Fra Alto e Pieno Medioevo*; Atti della giornata di studio, San Miniato, Italy, 1 December 2007; Firenze University Press: Florence, Italy, 2010; p. 184. Available online: https://books.fupress.com/catalogue/vico-wallari--san-genesio-ricerca-storica-e-indagini-archeologiche-su-una-comunit-del-medio-valdarno/1936 (accessed on 28 October 2022).
2. Dominici, S.; Mazzanti, R.; Nencini, C. Geologia dei dintorni di San Miniato tra l'Arno, l'Elsa e l'Era. *Quad. Mus. St. Nat. Livorno* **1995**, *14*, 1–27.
3. Mendera, M.; Cantini, F.; Mercante, F.; Silvestri, A.; Gallo, F.; Molin, G.; Pescarin Volpato, M. Where does the medieval glass from San Genesio (Pisa, Italy) come from? In Proceedings of the AIHV Annales du 20me Congrès, Fribourg/Romont, Switzerland, 7–11 September 2015; Verlag Marie Leidorf GmbH, Geschäftsführer: Rahden, Germany; pp. 360–365, ISBN 978-3-86757-024-4.
4. Viva, S.; Cantini, F.; Fabbri, P.F. Post mortem fetal extrusion: Analysis of a coffin birth case from an Early Medieval cemetery along the Via Francigena in Tuscany (Italy). *J. Archaeol. Sci. Rep.* **2020**, *32*, 102419. [CrossRef]
5. Cantini, F.; Viva, S.; Marani, F. La necropoli di seconda metà VI secolo di San Genesio (San Miniato-Pisa): Elementi endogeni ed esogeni. In *Dalle steppe al Mediterraneo, Popoli, Culture, Integrazione, Proceedings of the Atti del Convegno Internazionale di Studi, Fondazioni e Rituali Funerari Delle Aristocrazie Germaniche nel Contesto Mediterraneo, Cimitile-Santa Maria Capua Vetere*; Naples, Italy, 18–19 June 2015; Ebanista, C., Rotili, M., Eds.; Guida Editor: Naples, Italy, 2017; pp. 251–268. ISBN 978-88-6866-357-5.
6. Pavón-Carrasco, F.J.; Rodriguez-Gonzalez, J.; Osete, M.L.; Torta, J.M. A Matlab tool for archaeomagnetic dating. *J. Archaeol. Sci.* **2011**, *38*, 408–419. [CrossRef]
7. Pavón-Carrasco, J.F.; Osete, M.L.; Torta, M.J. A geomagnetic field model for the Holocene based on archaeomagnetic and lava flow data. *Earth Planet. Sci. Lett.* **2014**, *388*, 98–109. [CrossRef]
8. Pavón-Carrasco, J.F.; Gómez-Paccard, M.; Hervé, G.; Osete, M.L.; Chauvin, A. Intensity of the geomagnetic field in Europe for the last 3 ka: Influence of data quality on geomagnetic field modeling. *Geochem. Geophys. Geosyst.* **2014**, *15*, 2515–2530. [CrossRef]

9. Pavón-Carrasco, F.J.; Campuzano, S.A.; Rivero-Montero, M.; Molina-Cardín, A.; Gómez-Paccard, M.; Osete, M.L. SCHA.DIF.4k: 4000 Years of Paleomagnetic Reconstruction for Europe and Its Application for Dating. *J. Geophys. Res. Solid Earth* **2021**, *126*, e2020JB021237. [CrossRef]
10. Schnepp, E.; Worm, K.; Scholger, R. Improved sampling techniques for baked clay and soft sediments. *Phys. Chem. Earth* **2008**, *33*, 407–413. [CrossRef]
11. Thellier, E. Sur la direction du champ magnétique terrestre en France durant les deux dernières millénaires. *Phys. Earth Planet. Int.* **1981**, *24*, 89–132. [CrossRef]
12. Le Goff, M. *Inductomètre à Rotation Continue Pour la Mesure des Faibles Aimantations Rémanentes et Enduites en Magnétisme des Roches, Mém. Diplôme d'Ingénieur*; CNAM: Paris, France, 1975.
13. Thellier, E.; Thellier, O. Sur l'intensité du champ magnétique terrestre dans le passé historique et géologique. *Ann. Geophys.* **1959**, *15*, 285–376.
14. McFadden, P.L. Rejection of palaeomagnetic observations. *Earth Planet. Sci. Lett.* **1982**, *61*, 392–395. [CrossRef]
15. Ficher, R.A. Dispersion on a sphere. *Proc. R. Soc. London (A)* **1953**, *217*, 295–305.
16. Mcintosh, G.; Catanzariti, G. An introduction to archaeomagnetic dating. *Geochronometria* **2006**, *25*, 11–18.
17. Malfatti, J.; Principe, C.; Gattiglia, G. Archaeomagnetic investigation of a metallurgic furnace in Pisa (Italy). *J. Cult. Herit.* **2011**, *12*, 1–10. [CrossRef]
18. Bucur, I. The direction of the terrestrial magnetic field in France during the last 21 centuries. *Phys. Earth Planet. Inter.* **1994**, *87*, 95–109. [CrossRef]
19. Coe, R.S. Paleo-intensities of the earth's magnetic field determined from tertiary and quaternary rocks. *J. Geophys. Res.* **1967**, *72*, 3247–3262. [CrossRef]
20. Coe, R.S.; Grommé, S.; Mankinen, E.A. Geomagnetic paleointensities from radiocarbon-dated lava flows on Hawaii and the question of the Pacific nondipole low. *J. Geophys. Res.* **1978**, *83*, 1740–1756. [CrossRef]
21. Chauvin, A.; Garcia, Y.; Lanos, P.; Laubenheimer, F. Paleointensity of the geomagnetic field recovered on archaeomagnetic sites from France. *Phys. Earth Planet. Inter.* **2000**, *120*, 111–136. [CrossRef]
22. Morales, J.; Goguitchaichvili, A.; Acosta, G.; González-Morán, T.; Alva-Valdivia, L.; Robles Camacho, J.; Hernández-Bernal, M.S. Magnetic properties and archeointensity determination on Pre-Columbian pottery from Chiapas, Mesoamerica. *Earth Planets Space* **2009**, *61*, 83–91. [CrossRef]
23. Dunlop, D.J.; Özdemir, Ö. *Rock Magnetism. Fundamentals and Frontiers*; Cambridge Studies in Magnetism Series; Cambridge University Press: Cambridge, UK, 1997; pp. 1–573.
24. Goguitchaichvili, A.; Morales, J.; Urrutia-Fucugauchi, J. On the use of continuous thermomagnetic curves in paleomagnetism. *C. R. Acad. Sci. Earth and Planet. Sci.* **2001**, *11*, 699–704.
25. Principe, C.; Malfatti, J. Giuseppe Folgheraither: The Italian pioneer of archaeomagnetism. *Earth Sci. Hist.* **2020**, *39*, 305–335. [CrossRef]
26. Riccomi, G.; Minozzi, S.; Zech, J.; Cantini, F.; Giuffra, V. Stable isotopic reconstruction of dietary changes across Late Antiquity and the Middle Ages in Tuscany. *J. Archaeol. Sci. Rep.* **2020**, *3*, 102546. [CrossRef]
27. Viva, S.; Lubritto, C.; Cantini, F.; Fabbri, P.F. Evidence of Barbarian migrations and interpersonal violence during the Gothic War in sixth-century Tuscany: The case of the Goth horseman from San Genesio (Pisa). *Archaeol. Anthropol. Sci.* **2022**, *14*, 39. [CrossRef]